JOURNAL OF EXPERIMENTAL AND THEORETICAL PHYSICS, 2024, Vol. 165, No. 6, pp. 859–867

STATISTICAL, NONLINEAR, AND SOFT MATTER PHYSICS

NONLINEAR OSCILLATIONS OF POORLY CONDUCTING LIQUID IN ALTERNATING ELECTRIC FIELD IN THE FRAMEWORK OF LOW-MODE APPROXIMATION

© 2024 O.O. Nekrasov*, N.N. Kartavykh**

Perm State University 614068, Perm, Russia
** e-mail: dakeln2@gmail.com*
*** e-mail: kartavykh@psu.ru*

Received January 30, 2023
Revised February 25, 2024
Accepted February 25, 2024

Abstract. Flat horizontal infinite layer of viscous incompressible poorly conducting liquid is investigated. The layer is placed in gravitational and electric field and heated from above. Eight-mode electroconvection model (extended Lorenz-model) is used to carry the problem out numerically. As a result of the linear stability analysis of the system, the critical wave number and critical electric Rayleigh number are obtained for different external electric field periods. In the case of nonlinear evolution of the system, bifurcation diagrams are obtained as dependences of the dimensionless heat flow on the amplitude of the oscillations of the external electric field. Various types of system response to the external impact are found: periodic, quasiperiodic and chaotic oscillations, as well as hysteretic transitions between them and quiescent state. The map of flow regimes is obtained.

Keywords: *electroconvection, low-mode model, electroconductive charge formation, oscillations, alternating electric field, hysteresis*

DOI: 10.31857/S004445102406e129

1. INTRODUCTION

Currently, the problem of controlling heat flux in continuous media, for example, in fluids, is relevant. The ability to control heat and mass transfer in fluids can be used in various technological applications: in designing effective heat removal systems or for process control in zero gravity [1–3].

The problem of thermogravitational mechanism of convection generation, when motion in non-uniformly heated fluid occurs due to buoyancy force, has been very well studied [4]. In this case, the fluid can possess a number of other physical properties, for example, it can be a carrier of free charge. In this case, there appears an additional way to control convective motion by affecting the fluid through the application of an external electric field [5, 6]. It is known that such influence can lead to changes in convection onset thresholds [6–9], to the generation of oscillatory [10] and chaotic [11] motion regimes.

This article examines the case of interaction between two convection mechanisms: thermogravitational and electroconductive [6, 9], associated with inhomogeneous conductivity distribution.

There are many approaches to studying the dynamics of nonlinear systems, most of which reduce to the application of numerical methods. The main difficulty is related to the absence of analytical solutions in the general form of the Navier–Stokes equations describing the behavior of viscous fluid.

In the mid-20th century, E. Lorenz demonstrated a new method of numerical modeling of the Navier-Stokes equations, based on studying the amplitudes of system field decomposition using a small set of trial functions [12]. In this convection model, the

phase variables are time-dependent amplitudes of spatial trigonometric functions (modes), one for the velocity field and two for temperature.

This approach revealed new important patterns in the behavior of dynamical systems and led to the creation of a new branch of physics – the theory of dynamical chaos [13]. Despite the intensive use of numerical models and commercial computational packages, low-mode systems are still used to analyze the nonlinear evolution of flows in various fluids [14–17], including the initial stage of laminar-turbulent transition [14]. The use of low-mode models for theoretical description of convection in variable fields shows good agreement with experiments even for large supercriticalities [18,19].

In this work, a modified Lorenz model is used to analyze electrothermo-convective flows, based on the decomposition of hydrodynamic system fields into eight basis functions reflecting the symmetry of the problem [10, 20]. Within the framework of the proposed model, cases of instantaneous and finite-time charge relaxation have been studied for heating of weakly conducting fluid from below in a constant electric field [20], in the isothermal case and with strong heating from above in an alternating electric field [9]. This paper presents the results of studying the evolution of weakly conducting fluid flows arising in an alternating electric field with moderate heating from above. New sequences of transitions between regular and chaotic oscillatory flows have been discovered and analyzed.

2. PROBLEM STATEMENT

A flat infinite horizontal layer of viscous incompressible weakly conducting fluid of thickness h, placed between plates of a flat infinite horizontal capacitor, is considered. The fluid is subjected to an alternating electric field with intensity E, gravitational field g, and the capacitor plates are heated to a temperature difference Θ. The capacitor plates are perfectly heat and electrically conductive, with physical conditions on them expressed by the following relations:

$$z = 0 : \hat{T} = \Theta, \Phi = \hat{U}\cos(\omega t), \qquad z = h : \hat{T} = 0, \Phi = 0, \tag{1}$$

where z is the vertical coordinate, ω is the frequency of the external electric field, $\hat{U}$ is the amplitude of electric potential variation Φ.

A weakly conducting fluid is defined as having electrical conductivity $\sigma \sim 10^{-9}$–$10^{-11}\,\mathrm{Ohm}^{-1}\cdot\mathrm{m}^{-1}$, which allows using the electrohydrodynamic approximation: due to small currents, magnetic effects and Joule heating can be neglected [6, 7].The system of differential equations describing the system includes the Navier–Stokes equation, heat conduction equation, charge conservation law, Gauss's law, relation between electric field intensity and its potential, continuity equation [21]:

$$\rho\left(\frac{\partial \boldsymbol{v}}{\partial t} + (\boldsymbol{v}\times\nabla)\boldsymbol{v}\right) = -\nabla p + \rho\boldsymbol{g} + \eta\Delta\boldsymbol{v} + q\boldsymbol{E},$$

$$\frac{\partial \hat{T}}{\partial t} + (\boldsymbol{v}\times\nabla)\hat{T} = \chi\Delta\hat{T},$$

$$\frac{\partial q}{\partial t} + div(\sigma\boldsymbol{E}) + (\boldsymbol{v}\times\nabla)q = 0, \tag{2}$$

$$div\boldsymbol{E} = q/\varepsilon\varepsilon_0,$$

$$\boldsymbol{E} = -\nabla\Phi,$$

$$div\boldsymbol{v} = 0,$$

where $\mathbf{v}, p, \hat{T}$ are velocity, pressure, and temperature fields respectively, η is fluid dynamic viscosity, ρ is fluid density, q is fluid density, σ is fluid electrical conductivity, ε is dielectric permittivity, ε_0 is electric constant.

Linear dependencies of fluid density and electrical conductivity on temperature are considered:

$$\rho = \rho_0(1 - \beta_\rho\hat{T}), \quad \sigma = \sigma_0(1 + \beta_\sigma\hat{T}),$$

see [6,21], where ρ_0 and σ_0 are density and conductivity values at mean temperature, β_θ and β_σ are positive coefficients. Thus, thermogravitational and electroconductive mechanisms are the main causes of convection onset [9]. Due to small conductivity inhomogeneity (for weakly conducting fluid under moderate heating $\beta_\sigma\hat{T} \ll 1$), spatial inhomogeneity of the electric field and field changes caused by charge redistribution can be neglected, i.e., the induction-free approximation can be used [20].

System (2) is reduced to dimensionless form according to the following relations:

$$[t] = \frac{\chi_0 h^2}{\kappa}, [F] = \hat{U}, [v] = \frac{\chi}{\kappa}, [r] = h,$$
$$[\hat{T}] = Q, E = \frac{\hat{U}}{h}, [p] = \frac{\kappa\chi}{h^2}, [q] = \frac{\varepsilon\varepsilon_0\hat{U}}{h^2}, \quad (3)$$

and considering the Boussinesq approximation [4], it can be written as

$$\frac{\partial \mathbf{v}}{\partial t} + \frac{1}{\mathrm{Pr}}(\mathbf{v}\nabla)\mathbf{v} =$$
$$= -\nabla p + \Delta\mathbf{v} + Ra\hat{T}\mathbf{j} + Ra_s q\cos(\omega t)\boldsymbol{j},$$
$$\mathrm{Pr}\frac{\partial \hat{T}}{\partial t} + (\mathbf{v}\nabla)\hat{T} = \Delta\hat{T}, \quad (4)$$
$$\mathrm{Pr}_e\frac{\partial q}{\partial t} + div(\sigma\mathbf{E}) + \frac{Pr_e}{Pr}(\mathbf{v}\nabla)q = 0,$$

where j is a unit vector codirectional with the vertical z-axis. System (4) contains the following dimensionless parameters:

$$Ra = \frac{\chi_0 g\beta_\rho Q h^3}{\chi\kappa}$$

— Rayleigh number, characterizing the intensity of fluid heating,

$$Ra_s = \frac{\varepsilon_0\varepsilon\hat{U}^2\beta_s Q}{\chi\kappa}$$

— electrical analog of the Rayleigh number, related to the amplitude of the external electric field,

$$Pr = \frac{\kappa}{\chi\chi_0}$$

— Prandtl number, reflecting the ratio between viscous and heat-conductive energy transfer in the fluid,

$$\mathrm{Pr}_e = \frac{\varepsilon\varepsilon_0\kappa}{h^2\sigma_0\chi_0}$$

— electrical analog of the Prandtl number, characterizing the ratio between viscous and electrical forces.

3. LOW-MODE MODEL

Let's represent the fields $v, \hat{T}$ and q in the form $v, \hat{T} = \hat{T}_0 + \theta$ and $q = q_0 + q\varphi$, where v, θ and $q\varphi$ are deviations of values from their equilibrium values (hereafter primes will be omitted). Considering the absence of horizontal anisotropy, we can consider only two-dimensional perturbations in the vertical plane $x - z$, which actually arise at the threshold of convective stability. Let's introduce the stream function ψ, such that

$$v_x = -\partial\psi / \partial z, \quad v_z = \partial\psi / \partial x,$$

see [9], then the system of equations (4) can be rewritten as [20]

$$\frac{\partial}{\partial t}\Delta\psi + \frac{1}{\mathrm{Pr}}\left(\frac{\partial\psi}{\partial x}\frac{\partial}{\partial z}\Delta\psi - \frac{\partial\psi}{\partial z}\frac{\partial}{\partial x}\Delta\psi\right) = \Delta^2\psi +$$
$$+ Ra\frac{\partial\theta}{\partial x} + Ra_s\frac{\partial q}{\partial x}\cos(\omega t),$$
$$\mathrm{Pr}\frac{\partial\theta}{\partial t} + \frac{\partial\psi}{\partial x}\frac{\partial\theta}{\partial z} - \frac{\partial\psi}{\partial z}\frac{\partial\theta}{\partial x} = \Delta\theta + \frac{\partial\psi}{\partial x}, \quad (5)$$
$$\mathrm{Pr}_e\frac{\partial q}{\partial t} + \frac{\mathrm{Pr}_e}{\mathrm{Pr}}\left(\frac{\partial\psi}{\partial x}\frac{\partial q}{\partial z} - \frac{\partial\psi}{\partial z}\frac{\partial q}{\partial x}\right) +$$
$$+ q + \frac{\partial\theta}{\partial z}\cos\omega t = 0,$$

with boundary conditions

$$z = 0: \psi = \psi_{zz} = \theta = 0,$$
$$z = h: \psi = \psi_{zz} = \theta = 0. \quad (6)$$

To find solutions of the system of equations (5) satisfying boundary conditions (6), the Galerkin method [4] is applied with approximation of fields ψ, θ and q by a minimal set of basis functions [9]:

$$\psi = \frac{\sqrt{2}(1+k^2)}{k},$$
$$\times (X(t)\sin\pi z + V(t)\sin 2\pi z)\sin\pi kx,$$
$$\theta = \frac{\sqrt{2}}{\pi}(Y(t)\sin\pi z + W(t)\sin 2\pi z)\cos\pi kx +$$
$$+ \frac{1}{\pi}Z(t)\sin 2\pi z, \quad (7)$$

$$q = (\sqrt{2}S(t)\cos pz + 2\sqrt{2}T(t)\cos 2pz)\cos pkx + \\ + U(t)\cos 2pz.$$

Here k is the wave number characterizing the periodicity of solutions horizontally, and coefficients X, V, Y, W, Z, S, T, U are amplitudes showing the contribution of spatial modes to the solution.

Expansions (7) contain terms of different parity in z, which is related to the presence of derivatives of different orders in in system (5). Amplitudes X - U are determined using conditions expressing the orthogonality of the residual of system equations (5) with respect to each of the basis functions [4]. After time rescaling

$$t \to \frac{\mathrm{Pr}}{p^2(1+k^2)}t$$

we obtain a system of eight ordinary differential equations for the amplitudes of spatial harmonics (dot above variable denotes time derivative) [9,22]:

$$\dot{X} = \mathrm{Pr}(-X + rY - eT\cos wt),$$

$$\dot{Y} = -Y + X + XZ,$$

$$\dot{Z} = -bZ - XY,$$

$$\dot{V} = \mathrm{Pr}(-dV + (rW + eS\cos wt)/d), \qquad (8)$$

$$\dot{W} = -dW + V,$$

$$\dot{S} = -gS + XU - gY\cos wt,$$

$$\dot{T} = -gT - gW\cos wt,$$

$$\dot{U} = -gU - XS - 2gZ\cos wt.$$

In system (8), the following notations are introduced:

$$r = \frac{Ra}{Ra_0}, e = \frac{Ra_s}{Ra_{s0}},$$

$$Ra_0 = \frac{p^4(1+k^2)^3}{k^2}, Ra_{s0} = \frac{3p^4(1+k^2)^3}{8k^2}, \qquad (9)$$

$$d = \frac{4+k^2}{1+k^2}, b = \frac{4}{1+k^2}, g = \frac{\mathrm{Pr}}{p^2(1+k^2)\mathrm{Pr}_e},$$

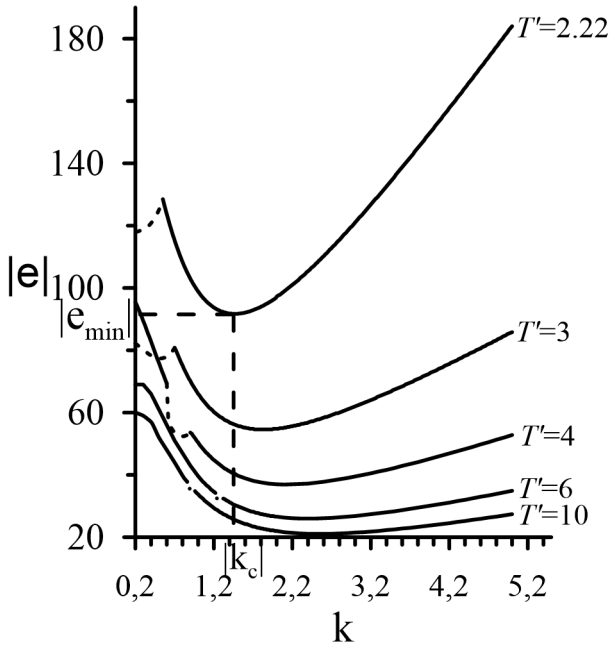

Fig. 1. Family of neutral curves in coordinates wave number k – modulus of electrical parameter |e| at different periods T' of external electric field variation. Solid lines correspond to quasi-periodic regimes, dashed lines to synchronous ones [23]

where r, e — are normalized thermal and electrical Rayleigh numbers, Ra_0 — is the critical Rayleigh number at which thermogravitational convection begins, Ra_{s0} is the system parameter.

4. LINEAR STABILITY ANALYSIS

The case of moderate heating from above is studied, where the normalized thermal Rayleigh number r takes a negative value of -1 [23]. As seen from relations (9), with heating from above, the normalized electric Rayleigh number is e also negative, but the study considered its absolute value. Other fluid parameters have values $Pr = 400, Pr_e = 30$. They correspond to weakly conducting fluids, electrical conductivity of which depends on temperature, for example, corn or transformer oil [24–26]. Real physical characteristics of the system correspond to a layer thickness of 1 cm, voltage difference of 1 kV, temperature difference: ~10°C.

As seen from system (8) with a set of dimensionless parameters (9), the wave number k, corresponding to the spatial horizontal scale of perturbations, remains undetermined. The standard approach for finding

the value of this parameter is the analysis of linear perturbations of the system.

After linearization, system (8) can be represented in matrix form

$$\dot{\mathbf{x}}(t) = A(t)\mathbf{x}(t)$$

with a linear matrix dependent on time with period $T\text{¢} = 2\text{p} / \text{w}$. Then for analysis of its linear stability, Floquet theory can be applied [27], which was used to obtain neutral curves of linear stability of the system for different periods of external electric field (Fig. 1) [23].

By determining the extremum point of the neutral curve, one can calculate the minimum modulus value of the dimensionless electric parameter at which convective fluid motion begins, as well as the corresponding critical wave number, for example, $|e_{min}|(T\text{¢} = 2.22) = 91.7$ and $k_c(T\text{¢} = 2.22) = 1.45$. Linear stability analysis of the system predicts the emergence of quasi-periodic oscillations in areas of global minimum of neutral curves Fig. 1. In areas of local minima of curves, oscillations are synchronous, corresponding areas are constructed with dashed lines.

5. NONLINEAR CONVECTION MODES

To describe the intensity of convective processes, the Nusselt number (Nu) was calculated, a parameter equal to the time-averaged heat flux per unit of horizontal boundary of the condenser [9]. The Nusselt number can be expressed through the amplitude Z of system (8):

$$Nu = 1 - \frac{2}{t_{end}} \int_0^{t_{end}} Z(t)dt, \qquad (10)$$

where t_{end} is chosen in such a way that it accommodates more than a hundred periods of system oscillations.

Wave numbers k were taken from the results of linear theory application ($k = k_c$, where k_c corresponds to the global minimum of the neutral curve for the selected period of external field). Geometric parameters b, g and d were determined based on the selected wave number. Values of other dimensionless parameters are given at the beginning of Section 4.

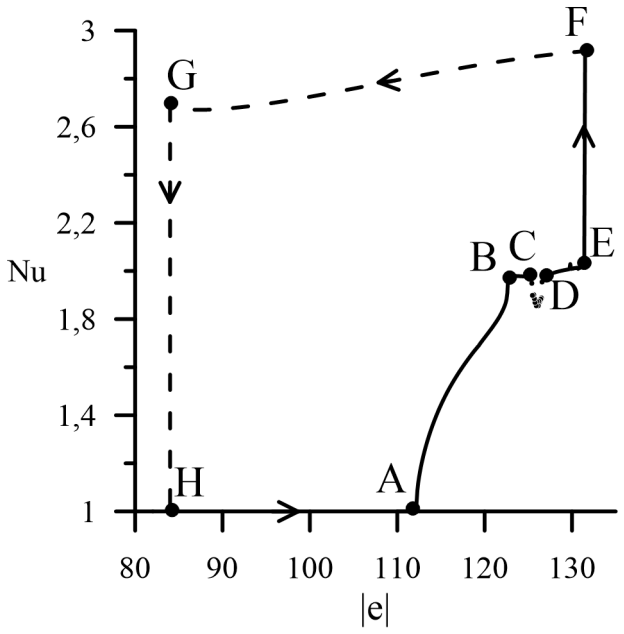

Fig. 2. Dependence of the Nusselt number Nu on the absolute value of the dimensionless electric parameter |e| at external field period $T' = 2$. Solid line – movement towards increasing |e|, dashed line – towards decreasing |e|

The study of electroconvection modes was conducted as follows: system (8) was numerically integrated using the fourth-order Runge-Kutta method at different values of dimensionless normalized electric Rayleigh number |e| and period of electric field variation T'. The |e| parameter continuation method was used: when calculating the Nusselt number for each value, distributions obtained at the previous step for were used as initial conditions |e|. This method allows continuous change of the control parameter, determining the boundaries of hysteresis transitions [28]. Thus, dependencies Nu (|e|) were determined for different periods of external electric field T', for each period the corresponding critical wave number value was taken.

During the study, several types of system evolution were identified for different periods of external field $T\text{¢}$.

5.1. External field period $T' = 2$

The dependence of dimensionless heat flux Nu on parameter |e| for the given period of external field is presented in Fig. 2.

With increasing parameter |e| from initial conditions corresponding to small perturbations of mechanical equilibrium, convection emerges as quasi-periodic oscillations at point A Fig. 2

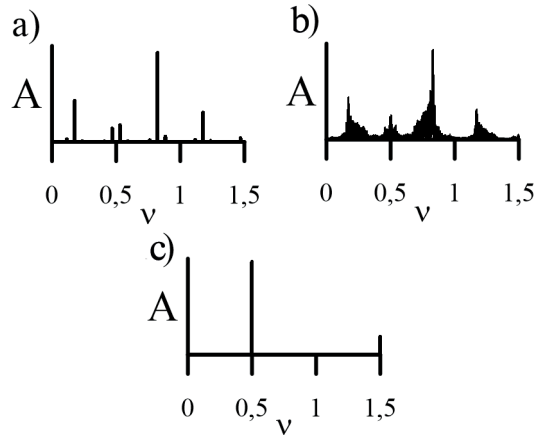

Fig. 3. Fourier spectra of amplitude oscillations X at forcing period for different values of $T' = 2$. Lower branch of Fig. 2: *a* — |e| = 120, quasiperiodic response; *b*, |e| = 126 chaotic oscillations. Upper branch of Fig. 2: *c*, |e| = 131 synchronous response

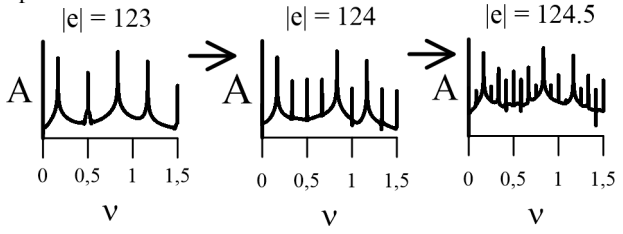

Fig. 4. Fourier spectra of amplitude oscillations X in logarithmic scale at forcing period $T' = 2$. Oscillations correspond to section BC of Fig. 2, where subharmonic cascade occurs

(|e| = 112.2) (the Fourier spectrum of amplitude oscillations contains two or more frequencies incommensurable with the external one (ν = 0.5, Fig. 3*a*)) .

With further increase of the parameter |e| quasiperiodic oscillations transition at point B Fig. 2 (|e| = 122.7) into a specific subharmonic oscillation regime: the Fourier spectrum contains the external frequency, as well as a frequency three times lower than the external one, and their linear combinations (Fig. 4).

In the BC section, a cascade of period-doubling bifurcations occurs (Fig. 4), transitioning into chaos at point C Fig. 2 (|e| = 124.7). Chaotic oscillations exist in the CD section of Fig. 2 and are characterized by a continuous Fourier spectrum (Fig. 3*b*). At point D Fig. 2 (|e| = 126.6) a regime emerges again, characterized by a frequency three times lower than the external field frequency.

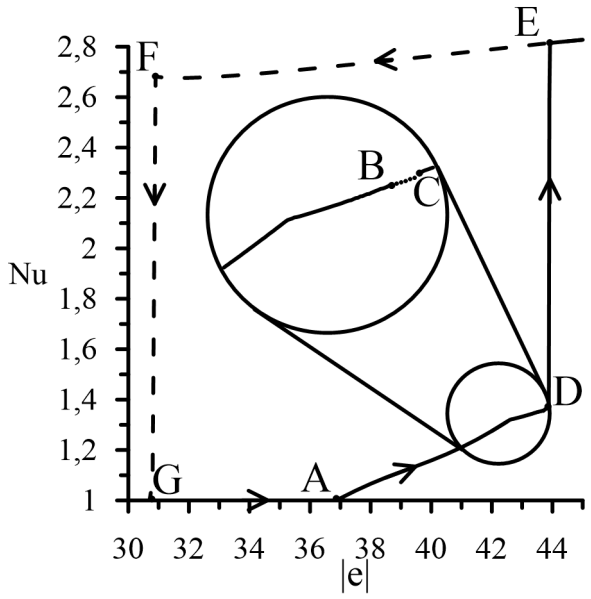

Fig. 5. Dependence of the Nusselt number Nu on the absolute value of the dimensionless electric parameter |e| at the external field period $T' = 4$. Solid line - movement towards increasing , dashed line – towards decreasing of |e|

With further increase of |e| the system oscillates in this way until point E Fig. 2 (|e| = 122.7), where heat flow sharply increases. At Nusselt numbers greater than 2.5, synchronous disturbances appear in the layer, whose Fourier spectra contain only frequencies that are multiples of the external one (Fig. 3*c*).

If, using the parameter continuation method, parameter |e| is sequentially decreased from values lying to the right of point F Fig. 2, then the system's transition from convective flow to mechanical equilibrium will occur differently, with a sharp decrease in the Nusselt number at point G Fig. 2 (|e| = 84). Thus, hysteresis is realized in the system (loop HAFG in Fig. 2), accompanied by heat flow jumps.

5.2 External field period $T' = 4$

The dependence of dimensionless heat flux on parameter |e| for the given external field period is shown in Fig. 5.

With increasing absolute value of parameter |e| convection occurs at point A Fig. 5 (|e| = 36.9) in the form of quasi-periodic oscillations. With further increase of |e| these oscillations transition to chaos through quasi-periodicity at point B Fig. 5 (|e| = 43.5). The transition to chaos through quasi-periodicity is

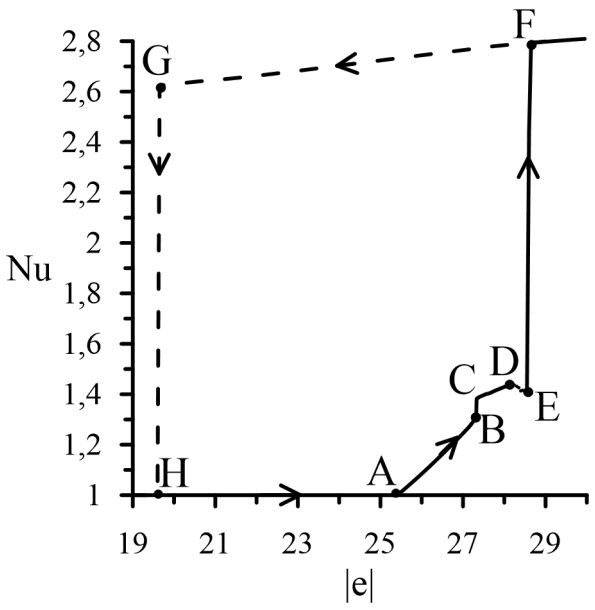

Fig. 6. Dependence of the Nusselt number Nu on the absolute value of the dimensionless electric parameter |e| at the external field period $T' = 6.2$. Solid line – movement towards increasing |e|, dashed line – towards decreasing |e|

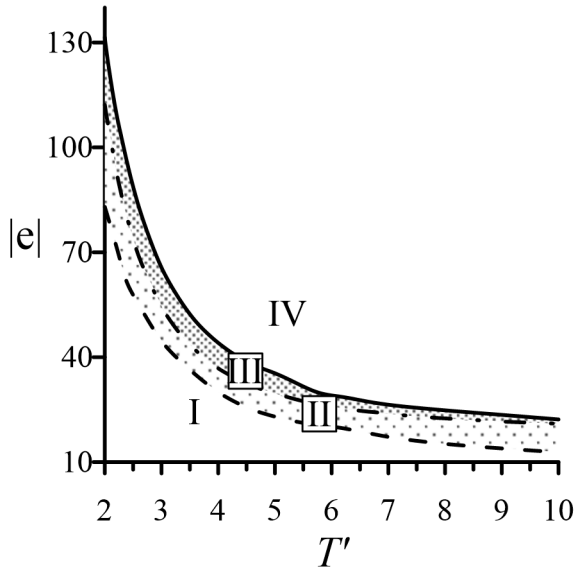

Fig. 7. Map of fluid motion regimes on the plane of external electric field period variation T' – absolute value of electric parameter |e|. I – region of no convection; II – region of coexistence of synchronous oscillations and no convection; III – region of coexistence of synchronous oscillations and various regimes: quasi-periodic oscillations, subharmonic oscillations, and chaos; IV – region of synchronous oscillations

accompanied by the appearance of an increasing number of linear frequency combinations incommensurable with the external one, until the spectrum becomes continuous. Chaos exists in section BC Fig. 5 (at point C ($|e| = 43.78$)). In section CD Fig. 5, a synchronization region is realized, where subharmonic oscillations are observed. Then, at point D Fig. 5 ($|e| = 43.9$) the heat flux experiences a sharp jump, and the system transitions to synchronous oscillations.

Similar to the previous case, hysteresis phenomenon is observed (loop ADEFG in Fig. 5): simultaneous coexistence of regimes with different Nusselt numbers. At $Nu > 2.6$ synchronous oscillations are realized (section EF in Fig. 5). When parameter |e| decreases at point F Fig. 5 ($|e| = 30.9$) the system transitions to equilibrium state.

5.3. External field period $T' = 6.2$

The dependence of dimensionless heat flux on parameter $|e|$ for the given external field period is shown in Fig. 6.

Similar to all previous cases, convection occurs in the form of quasi-periodic oscillations at point A Fig. 6 ($|e| = 25.4$). With increasing parameter at point B Fig. 6 ($|e| = 27.3$) a reverse bifurcation occurs (Nusselt number sharply increases for a certain value |e|), and the system transitions at point C Fig. 6 to oscillations characterized by a frequency three times lower than the external field frequency. Then a period-doubling cascade occurs, leading to the appearance of chaos at point D Fig. 6 ($|e| = 28.2$) which exists up to point E in Fig. 6 ($|e| = 28.6$), where the system transitions to synchronous oscillations with a sharp increase in the Nusselt number.

At this period of the external field, a hysteresis phenomenon is also observed (loop AEFGH in Fig. 6). On the upper branch of this loop FG Fig. 6, synchronous oscillations occur, and when synchronous oscillations occur, and when parameter e decreases at point G in Fig. 6 ($|e| = 19.6$), convection sharply disappears in the system

Based on the study of Nusselt number dependencies on the dimensionless electric parameter for different periods of external electric field variation, a map of electroconvection regimes was constructed for the period range [2; 10] (Fig. 7).

For all considered periods of external field variation, instability occurs with an increase in the control parameter |e| from the equilibrium state through

quasi-periodic oscillations (dash- dotted line in Fig. 7). With further increase in the electric Rayleigh number, low-intensity quasi-periodic oscillations can transform into subharmonic or chaotic regimes. With growth of the electroconvective parameter at the boundary marked by a solid line in Fig. 7, high-intensity synchronous oscillatory flows emerge. When decreasing the control parameter from regions of intense convection at the boundary marked by a dashed line in Fig. 7, transition to mechanical equilibrium of the fluid occurs.

CONCLUSION

The problem of electroconvection in a flat horizontal layer of viscous incompressible weakly conducting fluid placed in an alternating electric field and heated from above has been studied within the framework of a low-mode approximation. The case of moderate heating from above is considered.

As a result of studying linear perturbations under variable external influence, neutral curves depending on the electric field period were obtained, and corresponding critical wave numbers were determined.

In the nonlinear case, the evolution of the system under changes in amplitude and period of external electric field has been studied. Various types of system responses were discovered: quasi-periodic, subharmonic characterized by a frequency three times lower than the external forcing frequency, synchronous, and chaos. Different scenarios of transition to chaos were identified, through quasi-periodicity and through subharmonic cascade.

The phenomenon of hysteresis was discovered. Depending on initial conditions, oscillatory flows of weakly conducting fluid can have high or low intensity. The high-intensity regime corresponds to synchronous perturbations. For low-intensity oscillations, various system response modes are observed. Hysteresis transitions are accompanied by bifurcations. Linear theory predictions are confirmed in the nonlinear case.

FUNDING

This work was supported by the Russian Science Foundation (grant No. 23-21-00344, https://rscf.ru/project/23-21-00344/).

REFERENCES

1. V. S. Avduevskii, I. V. Barmin, S. D. Grishin et al., Cosmic Development Problems, Mashinostroenie, Moscow (1980).

2. V. I. Polezhaev, A. V. Bunet, N. A. Verezub el al., Mathematical Modelling of Convective Heat-masstransfer Based on the Navier-Stokes Equations, Nauka, Moscow (1987).

3. A. V. Getling, Rayleigh–Bénard Convection: Structures and Dynamics, Editorial URSS, Moscow (1999).

4. G. Z. Gershuni and E.M. Zhukhovitskii, Convective Stability of Incompressible Fluids, Nauka, Moscow (1976).

5. G. A. Ostroumov, Interaction of Electric and Hydrodynamic Fields. Physical Principles of Electrohydrodynamics, Nauka, Moscow (1979).

6. M. K. Bologa, F. P. Grosu and I. A. Kozhukhar', Electrical Convection and Heat Transfer, Sttintsa, Chisinau (1977).

7. B. L. Smorodin and M. G. Verlade, J. Electrostatics 48, 261 (2000).

8. V. A. Il'in, B. L. Smorodin, Technical Physics Letters 31, 57 (2005).

9. N. N. Kartavykh, B. L. Smorodin, V. A. Il'in, JETP 148, 178 (2015).

10. V. A. Il'in, B. L. Smorodin, Technical Physics Letters 33, 81 (2007).

11. B. L. Smorodin, A. V. Taraut, JETP, 180 (2014).

12. E. N. Lorenz, J. Atmosph. Sci. 20, 130 (1963).

13. P. Berge, I. Pomo, K. Bidal, Towards a Deterministic Approach to Turbulence, Mir, Moscow (1991).

14. N. B. Volkov, N. M. Zubarev, JETP 107, 1868 (1995).

15. J. Jawdat, Int. Commun. Heat Mass Transfer 37, 629 (2010).

16. D. Laroze, Commun. Nonlin. Sci. Numer. Simul. 18, 2436 (2013).

17. A. Srivastava and B. Bhadauria, J. Nanofluids 12, 904 (2023).

18. R. Finucane and R. Kelly, Int. J. Heat and Mass Transfer 19, 71 (1976).

19. G. Ahlers, P. C. Hohenbergm, and M. Luke, Phys. Rev. A 32, 3519 (1985).

20. V. A. Il'in, Technical Physics 83, 64 (2013).

21. L. D. Landau, E. M. Lifshitz, Theoretical Physics, vol. VI. Fluid Mechanics, Nauka, Moscow (1986).

22. B. Smorodin and N. Kartavykh, Micrograv. Sci. Technol. 32, 423 (2020).

23. O. O. Nekrasov and N. N. Kartavykh, Interfacial Phenomena and Heat Transfer 7, 217 (2019).

24. S. R. Kosvintsev, Perm University Herald, Physics 2, 128 (1994).

25. S. A. Zhdanov, S. R. Kosvintsev, I. Yu. Makarihin, JETP 117, 398 (2000).

26. S. R. Kosvintsev, B. L. Smorodin, S. A. Zhdanovet al., Proc. Int. Conf. Modern Problems of Electrophysics and Electrohydrodynamics of Liquids» (MPEEL), 79 (2000).

27. E. A. Coddington and N. Levinson, Theory of Ordinary Differential Equations, Foreign Languages Publishing House, Moscow (1958).

28. E. L. Tarunin, Computational Experiment in Free Convection Problems, Irkutsk University Publishing, Irkutsk (1990).